JACS
JOURNAL OF THE AMERICAN CHEMICAL SOCIETY

Article

pubs.acs.org/JACS

On an Easy Way To Prepare Metal–Nitrogen Doped Carbon with Exclusive Presence of MeN_4-type Sites Active for the ORR

Ulrike I. Kramm,*[,†,‡] Iris Herrmann-Geppert,[†] Jan Behrends,[§] Klaus Lips,[∥] Sebastian Fiechter,[†] and Peter Bogdanoff[†]

[†]Institute for Solar Fuels, Helmholtz-Zentrum Berlin für Materialen und Energie, Hahn-Meitner-Platz 1, 14109 Berlin, Germany

[‡]Chair on Catalysts and Electrocatalysts, Graduate School of Excellence Energy Science and Engineering, Departments of Materials and Earth Science and Chemistry, TU Darmstadt, Jovanka-Bontschits-Strasse 2, 64287 Darmstadt, Germany

[§]Berlin Joint EPR Laboratory (BeJEL), Department of Physics, Freie Universität Berlin, Arnimallee 14, 14195 Berlin, Germany

[∥]Berlin Joint EPR Laboratory (BeJEL), Institute of Nanospectroscopy, Helmholtz-Zentrum Berlin für Materialen und Energie, Albert-Einstein-Str. 15, 12489 Berlin, Germany

Supporting Information

ABSTRACT: Today, most metal and nitrogen doped carbon catalysts for ORR reveal a heterogeneous composition. This can be reasoned by a nonoptimized precursor composition and various steps in the preparation process to get the required active material. The significant presence of inorganic metal species interferes with the assignment of descriptors related to the ORR activity and stability. In this work we present a simple and feasible way to reduce the contribution of inorganic metal species in some cases even down to zero. Such catalysts reveal the desired homogeneous composition of MeN_4 (Me = metal) sites in the carbon that is accompanied by a significant enhancement in ORR activity. Among the work of other international groups, our iron-based catalyst comprises the highest density of FeN_4 sites ever reported *without* interference of inorganic metal sites.

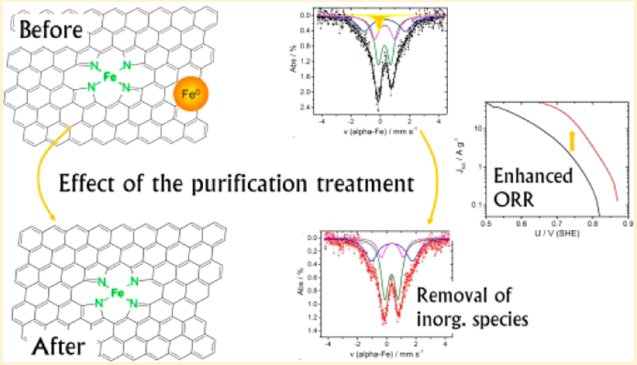

For commercialization of proton exchange membrane fuel cells (PEM FC), the fabrication costs have to be meaningfully reduced. Today, platinum-based catalysts are exclusively used in the fabrication process; however, they contribute by about 25% to the overall FC costs.[1] Recent publications have demonstrated promising catalytic activity and in some cases stability for oxygen reduction reaction (ORR) on metal and nitrogen doped carbon (Me–N–C) catalysts in PEM FC.[2−6] These findings were highly motivating for many groups to focus the research on this topic. Due to a basically good understanding of the preparation requirements, nowadays different preparation routes enable high ORR activity even in acidic electrolyte.[2−11] A question that was debated for a long period of time was the origin of ORR activity in these catalysts. In the best case, the catalyst should comprise only the presence of ORR active sites and carbon. However, structural characterization and the assignment of ORR activity to a specific structural motif in these catalysts is rather difficult. Therefore, techniques like X-ray absorption spectroscopy (XAS), time-of-flight secondary ion mass spectroscopy (TOF-SIMS), and Mößbauer spectroscopy (in the case of iron) are best suited.[12−35] As shown in Supporting Information Figure S1 a comparison of the XANES profile of different catalysts with the corresponding Mößbauer spectra indicates that the changes in the structural composition induced by the preparation conditions are much better reflected by Mößbauer spectroscopy compared to XANES where the profiles are almost identical. A further problem that has to be overcome is the fact that even today most of the Me–N–Cs are prepared without the utilization of an acid-leaching step.[3,8,20,28,30,31,36] However, as the active sites are formed during the heat-treatment of a metal–organic compound it is obvious that some side reactions can lead to the formation of inorganic metal species as it was observed for instance for the old INRS standard approach of Dodelet's group as published in our previous work.[31] If catalysts are characterized without acid-leaching often misleading conclusions on the origin of ORR activity were deduced.[37−43] In a recent publication it was concluded from in situ XANES data that an interaction of FeN_4/C-sites with metal particles is required in order to get high onset-potentials in acidic electrolyte.[44]

In our previous publications we were already able to elucidate a direct correlation of the ORR activity with the

Received: October 21, 2015
Published: December 10, 2015

DOI: 10.1021/jacs.5b11015
J. Am. Chem. Soc. 2016, 138, 635−640

iron content assigned to one specific FeN_4-site integrated in the pyrolytically formed carbon.[34] The catalysts discussed in our work were based on a synthesis route developed at the HZB in which porphyrines were pyrolyzed in the presence of iron oxalate and sulfur. After a final acid-leaching the obtained catalysts reveal high densities of active sites.[32,45−47] As a consequence in a cross laboratory comparison with other Me−N−Cs worldwide these catalysts reached the best ORR activities in RDE experiments.[8] The benefit of this HZB standard approach is that the obtained catalysts contain predominantly FeN_x-sites and only small quantities of metallic iron; so far, FeTMPPCl, iron oxalate, and sulfur are utilized in the preparation.[29,47] So far optimized in precursor ratio and heat-treatment conditions, also carbon-supported macrocycles will enable the preparation of predominantly FeN_x-sites. This allowed us the detailed study of the catalytic centers as a function of pyrolysis temperature. We were able to conclude that the electron density of a ferrous FeN_4-site in the low-spin state correlates with the turnover frequency for the ORR.[33] This site is also present in several catalysts prepared by alternative precursors.[3,6,7,11,28,30,31,48,49] However, direct correlations were usually hindered by significant contributions of inorganic iron species. In a very recent publication in *Nature Materials* some catalysts were synthesized free of inorganic iron species by keeping the metal content and the time of pyrolysis rather low.[35] Higher metal loadings (as, e.g., 1 wt % Fe in precursor) resulted in the formation of inorganic iron species.[35] Their finding was rather important as it confirms our previous assignment of ORR activity to the FeN_4 motif and excludes the requirement of additional metal particles to get good ORR activity. However, application of such low metal loadings is of course not of much interest for technical application due to low densities of active sites. So, demonstration of high onset-potentials for high metal-loading catalysts is required to fully clarify this issue.

Herein we present a method that enables the drastic reduction of inorganic metal species in Me−N−C catalysts by performing a second heat-treatment of as-synthesized catalysts in forming gas with a subsequent acid-leaching. This method is applicable even to catalysts with a high metal loading of >3 wt %, where the highest ORR activities are achieved so far.[2,3,6,8,11,35] After this purification treatment almost all inorganic byproducts are removed, and for catalysts prepared with iron oxalate and sulfur in the precursor only MeN_4-sites are present. Even more important is the result that the ORR activity is enhanced after this treatment and not decreased. This is in contradiction to the active site models reported by Hu et al. and Tylus et al. in which the inorganic metal particles were proposed as active site or as promoter for the ORR on MeN_4-sites, respectively, in acidic electrolyte.[44,50] This illustrates that metal particles are not required per se but could probably enhance the performance for catalysts prepared via some specific preparation routes.

The catalysts investigated in this work are based on the pyrolysis of porphyrins (CoTMPP and FeTMPPCl) together with metal oxalates (iron oxalate dihydrate or anhydrous tin oxalate). The pyrolysis temperature of catalysts prepared with tin oxalate was 750 °C, and the catalysts are labeled (Co,Sn) and (Fe,Sn), respectively, for CoTMPP and FeTMPPCl as precursor. The final heating temperature for catalysts prepared from porphyrin and iron oxalate was 800 °C. It should be noted that the latter catalysts were prepared under sulfur addition in order to gain the highest current densities.[29,47] These catalysts are labeled (Co,Fe) and $(Fe,Fe)_x$ (with CoTMPP and FeTMPPCl, respectively). For the preparation of the standard catalysts, the obtained pyrolysis product was subsequently acid-leached in hydrochloric acid. Details of the preparation route are given in the Supporting Information. The difference between the two Fe−N−C catalysts $(Fe,Fe)_1$ and $(Fe,Fe)_2$ is caused by utilization of ball-milled and as-obtained iron oxalate, respectively, as described in the experimental details in Supporting Information. The purification treatment reported in this work includes a second heat-treatment of the standard material in forming gas (N_2/10% H_2) with a subsequent further acid-leaching. The performance of this treatment is indicated by the addition of $+N_2/H_2$ to the sample label and leads to a significant reduction of inorganic metal species as illustrated below.

In Figure 1 the rotating disk electrode (RDE) curves (@ rpm 900) and the Tafel slopes of all catalysts prepared under the addition of iron oxalate are compared. Similar data for the samples prepared in the presence of tin oxalate are shown in Supporting Information Figure S2.

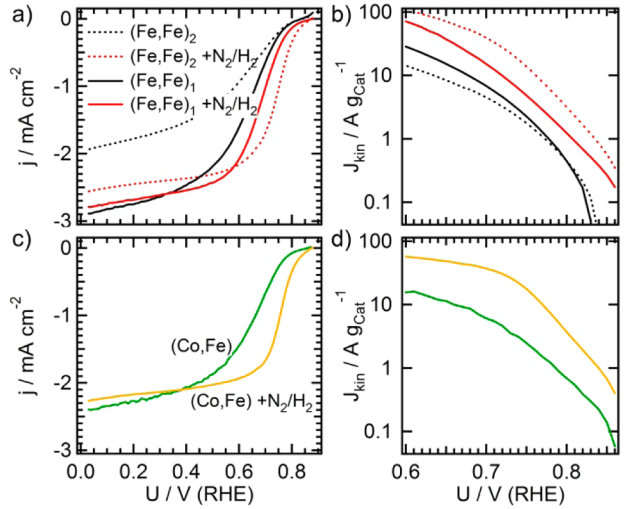

Figure 1. Results of the electrochemical measurements in 0.5 M H_2SO_4. Parts a and c show disc current densities for a rotation rate of 900 rpm, and parts b and d show kinetic current densities as a function of applied potential. Graphs are given for $(Fe,Fe)_1$, $(Fe,Fe)_2$, and (Co,Fe) catalysts before and after purifying treatment ($+N_2/H_2$).

In all cases a significant improvement in ORR activity was achieved. In Table 1 the onset-potential (determined for j = −0.1 mA cm^{-2}), the mass-related kinetic current density at 0.8 V, and the Tafel slopes are compared.

The following important conclusions can be made: The purification treatment leads always to a significant enhancement of the onset-potential and of the mass-related kinetic current density by factors between 3 and 10 whereas the Tafel slopes show only marginal and nonsystematic changes. The latter result let us conclude that the ORR mechanism is not changed by this purification treatment. In the following it will be shown that this enhancement is correlated with the significant reduction of inorganic metal species in the samples, as can be seen also from the comparison of the catalysts before and after purification in Table S2. Hence, participation of metal particles either as active site or assisting the ORR on MeN_4-sites as postulated by some authors can be excluded in our catalysts.[44,50]

DOI: 10.1021/jacs.5b11015
J. Am. Chem. Soc. 2016, 138, 635−640

Table 1. Summary of the Electrochemical Results Obtained in 0.5 M H_2SO_4

sample label		onset-potential U_{onset} (−0.1 mA cm^{-2})	mass-related kinetic current density J_k (0.8 V)/A g^{-1}	Tafel slope/mV/dec
$(Fe,Fe)_1$		0.83	0.45	68
	+N_2/H_2	0.875	1.23	78
$(Fe,Fe)_2$		0.835	0.45	79
	+N_2/H_2	0.88	3.15	68
(Co,Fe)		0.79	0.69	87
	+N_2/H_2	0.845	3.70	70
(Fe,Sn)		0.835	0.24	74
	+N_2/H_2	0.865	2.24	74
(Co,Sn)		0.825	0.82	59
	+N_2/H_2	0.85	2.30	59

Figure 2 compares Mößbauer spectra of the $(Fe,Fe)_1$ and $(Fe,Fe)_1$ + N_2/H_2 catalysts. For the fitting of the $(Fe,Fe)_1$

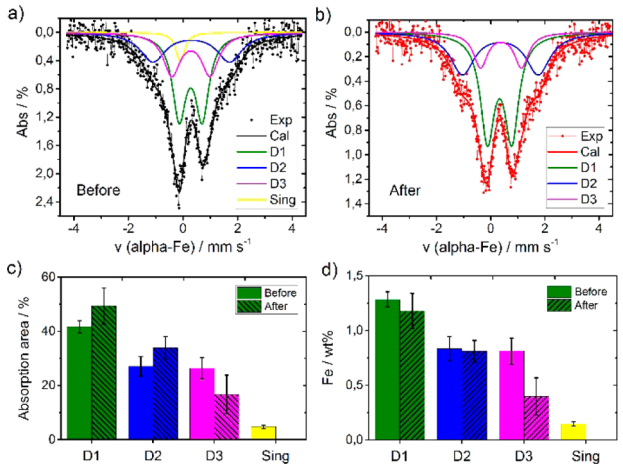

Figure 2. Mößbauer spectra of the $(Fe,Fe)_1$ catalyst (a, before) and the $(Fe,Fe)_1$ + N_2/H_2 (b, after) and change in the relative absorption area (c) and iron contents (d) induced by the purification treatment (+N_2/H_2). Assignment of Mößbauer sites to iron species is summarized in Table 2.

catalyst spectrum (before), three doublets and a singlet are required. After purification treatment only the doublets appear in the spectrum while the singlet vanishes. As the singlet is assigned to superparamagnetic iron, i.e., very small iron particles without magnetic ordering, this demonstrates the removal of the inorganic iron phases by the purification step.

The three doublets are assigned to FeN_4-sites that differ in their local environment leading to a ferrous low-spin (D1) and to two ferrous mid-spin (D2 and D3) sites. The main difference between these latter two sites is their local environment. While D3 has Mößbauer parameters similar to ferrous mid-spin porphyrins, D2 has Mößbauer parameters close to ferrous iron phthalocyanine (FePc). It is interesting to note that it is difficult to retain the ferrous mid-spin state in porphyrins under standard conditions. It seems that the carbon environment stabilizes this electronic state in our catalysts.

FePc has a rather unusual quadrupole splitting in comparison to other ferrous mid-spin FeN_4-sites. It is caused by the additional interaction of the iron center with nitrogen atoms which are integrated in the surrounding carbon yielding in a pseudo-octahedral coordination of the iron ion.[51] For our catalysts we also assume that the interaction in the axial direction leading to the doublet D2 is due to nitrogen. This pseudo-6-fold coordination of the Fe center by nitrogen might be the reason why this center does not contribute significantly to the ORR activity of porphyrin-based or alternatively prepared catalysts.[3,6,11,31,32,34,35,48]

In Figure 2c we calculated the content of iron assigned to each of the iron sites. This has to be done under the assumption of similar Lamb−Mößbauer factor that describe the recoil-free fractions. For the three FeN_4-sites we expect factors close to each other at room temperature (RT). As inorganic iron species usually reveal higher recoil-free fractions at RT, the content of the singlet might be overestimated. Nevertheless, in order to evaluate the changes in the absolute iron contents assigned to each site, this estimation is necessary and tolerable.

While the iron contents of the FeN_4-sites assigned to D1 and D2 remain constant, the superparamagnetic iron was completely leached out of the catalyst. In addition, the content of FeN_4-sites related to D3 was reduced by 50%. On first view, this purification treatment seems therefore more harmful to D3-based FeN_4-sites compared to others. Hence, while the carbon environment stabilizes its electronic structure in a first step, the purification treatment involving H_2 at high temperatures seems to cause a rearrangement to other electronic states or just destruction of these sites.

In addition, it has to be pointed out that the obtained concentration of FeN_4-sites *without* interference of inorganic iron species is by far the highest ever reported for Fe−N−C catalysts. It is significantly higher compared to that of the Fe−N−C catalyst reported by Zitolo et al. in *Nature Materials*.[35]

In Supporting Information Figure S3 the Mößbauer spectra of (Co,Fe) and (Co,Fe) + N_2/H_2 are compared to each other. In this case, beside the three doublets and the singlet sextet components were dominating the spectrum previous to the purification treatment. The sextets are assigned to iron nitride and α-iron. But again, after purification the spectrum reveals the presence of FeN_4-sites, only. (Note that, in this case, due to the dominance of the sextets in the as-prepared catalyst we did not determine the iron content assigned to each site, as the error would be too large.) The average Mößbauer parameters as well as the assignment to iron species is summarized in Table 2.

X-band electron pramagnetic resonance (EPR) spectroscopy of the $(Fe,Fe)_1$ and $(Fe,Fe)_1$ + N_2/H_2 catalysts together with X-ray diffraction (XRD) are given in Figure 3. XRD illustrates the X-ray amorphous behavior of the $(Fe,Fe)_1$ catalyst before and after purification treatment. This is a further indication that the iron particles present in the catalyst before purification treatment are rather small.

Also, for the other catalysts the metal contents were reduced, as illustrated by the X-ray diffractograms and transmission electron microscopy (TEM) images of the (Co,Sn) catalyst before and after purification in Supporting Information Figures S4 and S5. A significantly smaller fraction of crystalline phases is present after purification.

The assignment of our iron sites to ferrous species is further supported by the X-band EPR data. The X-band EPR spectrum of the $(Fe,Fe)_1$ catalyst in Figure 3a shows signal contributions assigned to ferric high- and mid-spin states. In general ferric

DOI: 10.1021/jacs.5b11015
J. Am. Chem. Soc. 2016, 138, 635−640

Table 2. Summary of the Mößbauer Parameters and Assignment to Iron Species for the Different Mößbauer Sites[a]

MS site	δ_{iso} / mm s^{-1}	ΔE_Q / mm s^{-1}	fwhm / mm s^{-1}	H_0 / T	Assignment
Sing	0.00 (0.14)	-	0.35 (0.07)	-	superparam. α-Fe
D1	0.32 (0.03)	0.81 (0.08)	0.63 (0.06)	-	$Fe^{II}N_4$-site, low-spin
D2	0.36 (0.04)	2.53 (0.33)	1.08 (0.30)	-	Pc-type $Fe^{II}N_4$-site, mid-spin
D3	0.35 (0.05)	1.36 (0.17)	0.69 (0.06)	-	Porph-type $Fe^{II}N_4$-site, mid-spin
Sext1	0.04 (0.02)	-	0.60 (0.01)	35.3 (0.2)	α-Fe
Sext2	0.34 (0.02)	-	1.13 (0.12)	48.3 (0.6)	iron nitride

[a]Errors are indicated in parentheses. The color code is similar to that used in Figure 2 and Supporting Information Figure S3.

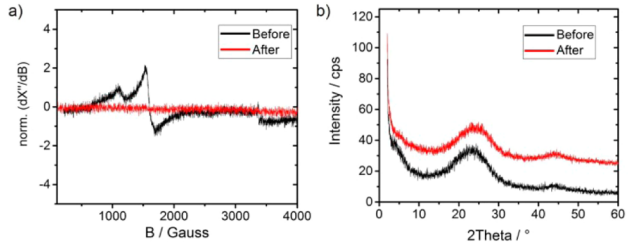

Figure 3. X-band EPR spectra (9.5 GHz) measured at 5 K (modulation amplitude: 1 mT/modulation frequency: 100 kHz) (a) and X-ray diffractograms (b) of the $(Fe,Fe)_1$ catalyst before and after $(+N_2/H_2)$ the purifying treatment.

high-spin FeN_4-sites can have Mößbauer parameters rather close to ferrous low-spin FeN_4-sites, so that we cannot distinguish between these two states just on the basis of Mößbauer parameters. However, the absence of both ferric contributions in the catalyst after purification in correlation with an increased catalytically activity indicates that the ORR active center must be a ferrous FeN_4-site. Obviously, the purification treatment removed all ferric species from our catalyst.

The same conclusion was drawn from catalysts which were prepared by pyrolysis of carbon-supported FeTMPPCl at 800 °C and a subsequent acid-leaching step. These samples have Mößbauer spectra similar to those of the above-discussed material (before purification) and do not show any Fe^{3+} contribution.[52] Hence, even in the standard catalyst only a minor fraction of ferric sites seems to be present.

In order to illustrate the significance of Mößbauer spectroscopy in comparison to XANES we also performed XANES measurements on the Fe−N−C catalysts. In Figure 4a the X-ray absorption near-edge spectroscopy (XANES) measurements obtained on the $(Fe,Fe)_1$ catalyst are shown before and after purification.

The relative intensities of the XANES profiles clearly illustrate the change in the iron concentration induced by the purification treatment step. A reduction of the iron concentration to 90% of the initial value is determined. This

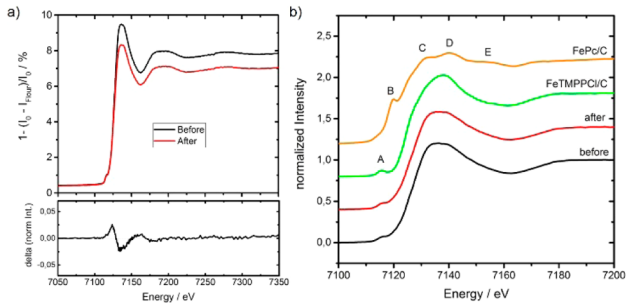

Figure 4. XANES profiles (a) of the $(Fe,Fe)_1$ catalyst before and after $(+N_2/H_2)$ the purifying treatment. In addition, the difference in the normalized XANES spectrum of both catalysts is shown at the bottom of part a. Normalized near-edge features of the same two catalysts and of reference samples, as indicated (b).

value is slightly higher than the one obtained from neutron activation analysis (NAA) of 80%, which is, however, the more reliable method for the determination of the all-over composition of a material.

For better evaluation of possible changes in the electronic structure of the catalysts by the purification step, the XANES profiles of both samples were normalized in a first step, and the difference curve was calculated in a second step. This difference curve is shown in Figure 4a (below) and reveals small changes basically in the range between 7120 and 7175 eV.

Figure 4b shows this energy range in more detail together with two reference samples, molecular FeTMPPCl and FePc, both impregnated on Ketjen Black 600.

XANES profiles of iron macrocycles usually exhibit several peaks (A−E) and sometimes a pre-edge feature P caused by the electronic interaction with neighboring atoms.[53] None of our catalysts or references reveal a pre-edge feature. Probably this is caused by the interaction with carbon in all cases.

In the relevant energy range the carbon-supported FePc reference exhibits several well-distinguished peaks (B, C, D). The B peak at 7119 eV is assigned to a dipole-allowed transition from metal 1s to 4p orbital. The C and D peaks at ∼7130 and ∼7140 eV, respectively, are related to multielectron scattering processes (i.e., interaction with neighboring atoms of first and second shell).[53] The carbon-supported FeTMPPCl reference exhibits only very broad and superimposed C and D peaks and an additional well-defined A-peak at 7115 eV.

For our catalyst a more or less unstructured XANES spectrum was obtained. The fact that the spectra are not well-resolved in our catalysts might be caused by the variation in the local environment of the individual iron atoms. It should be noted that the XANES profile just gives the average of all iron sites in the catalyst while the Mößbauer spectra in Figure 2 clearly indicate the presence of three distinguishable FeN_4-sites (and superparamagnetic iron for the Fe−N−C catalyst before purification treatment).

Only marginal undefined changes in the range of the C and D peaks can be observed for the catalyst after the purification step which does not allow a closer discussion or conclusions.

Most probably the changes in the spectra are caused by the relative contribution of the different iron sites which can be identified by Mößbauer spectroscopy (Figure 2) but not by XANES. Fitting the XANES profiles can give indication of the structural composition. Supporting information Figure S1 indicates, however, that the input on structural composition from other techniques is required. Hence, it is clear that the

DOI: 10.1021/jacs.5b11015
J. Am. Chem. Soc. 2016, 138, 635−640

Table 3. Comparison of the Metal Loadings, Kinetic Current Densities, and Estimated Turnover Frequencies of the Catalysts Described in this Work with those Reported by Zitolo and Jaouen et al. in Nature Materials[a]

	Fe/wt %	Fe(D1)/wt %	J(0.8 V)/A g_{Cat}^{-1}	TOF(0.8 V) e s^{-1} sites^{-1}
$(Fe,Fe)_1$	3.1	1.25	0.45	0.02
$(Fe,Fe)_1$ + N_2/H_2	2.4	1.2	1.23	0.06
0.5Fe	1.5	0.75	1.47	0.11
0.5Fe-900	1.2	0.6	3.42	0.33

[a]Details for the calculation of the iron loading and TOF for the catalysts described in *Nature Materials* are given in the Supporting Information.

change in structural composition induced by the purification treatment is significantly better illustrated by the Mößbauer spectra.

What is the reason for the enhanced ORR activity that accompanies the removal of inorganic iron species?

In a previous work we discussed the effect of a second heat-treatment (SHT) in different gas atmospheres on the ORR activity of (Fe,Fe) and (Fe,Co) catalysts (labeled Fe/Fe/S and Co/Fe/S in that work).[54] It was found that an enhancement of the surface area was at the origin of the enhanced catalytic activity. It should be pointed out that structural characterization of these catalysts subsequently heat-treated in N_2 and CO_2[34] or NH_3[32] did not cause a significant change of the contribution of inorganic iron species. This is clear for SHTs in N_2 and CO_2 as there none of the catalysts was subjected to a subsequent acid-leaching. Indeed, performing an additional acid-leaching after these SHTs caused a drop of the activity down to the values of the starting material (not published). In the case of NH_3 treatment[32] the activity remained on a high level even after the additional acid-leaching. We assume that part of the processes that are related to the SHT in NH_3 do apply here as well. This can easily be understood as part of the ammonia is decomposed to N_2 plus H_2 on iron particles that might be set free during the SHT. The main difference for the NH_3 treatment, however, is given by the fact that iron nitride species are formed during the SHT. Hence it is more difficult to optimize the process for complete removal of inorganic iron species.

On the basis of our previous experiences with other SHTs we propose the following mechanism for the removal of inorganic metal species induced by the purification treatment: (Step 1) The second heat-treatment in N_2/H_2 allows an increase of the surface area whereas inorganic metal particles come to the surface. (Step 2) Within the subsequent acid-leaching these particles are removed from the catalyst.

Also, recently we showed that beside the number of active sites, the surface area is an important factor for enhancing ORR activity.[3] As the content of the ORR active species in these catalysts stays practically constant, we conclude that most probably also here an enhanced surface area and hence better utilization of active sites[11] are at the origin of higher ORR activity after purification.

How do these catalysts compare to the metal-free Fe−N−C catalysts described by Zitolo and Jaouen et al. in *Nature Materials*?[35] In Table 3 the short labels, metal loadings, and estimates of the turnover frequencies (TOF) are summarized for the $(Fe,Fe)_1$ before and after purification and the two particle-free catalysts described in *Nature Materials* assuming that the main activity is attributed to the D1 doublet.[34]

The comparison of TOF values illustrates factors of 2 and 5 higher TOFs for 0.5Fe and 0.5Fe-900, respectively, in comparison to our $(Fe,Fe)_1$ + N_2/H_2 catalyst. With consideration of the known effects of pyrolysis temperature,[33] or ammonia treatment,[21,32] on the TOF of D1-related sites, these factors are within the expected range.

In conclusion our results demonstrate the successful removal of significant fractions of inorganic metal species from different types of Me−N−C catalysts. Three important aspects have to be highlighted: (1) In contrast to conclusions previously made by others the removal of metallic particles from the catalyst leads to a tremendous increase in ORR activity. (2) Mößbauer spectroscopy clearly indicates the presence of different FeN_4-sites while the XANES profile illustrates an average of the electronic environment of all iron atoms. (3) Our catalysts reach the highest concentration of FeN_4-sites ever reported *without* interference by inorganic metal species.

Hence, it is illustrated that the performance of a purification treatment in forming gas followed by a subsequent acid-leaching is in all terms beneficial for the catalysts.

■ ASSOCIATED CONTENT

Supporting Information

The Supporting Information is available free of charge on the ACS Publications website at DOI: 10.1021/jacs.5b11015.

Experimental details, Mößbauer and XANES profiles, RDE data of tin-oxalate-based catalysts, Mößbauer spectra of the (Co,Fe) before and after purification, and XRD and TEM images of the (Co,Sn) catalyst before and after purification with discussion related to calculation of the parameters for the catalysts described in ref 35 (PDF)

■ AUTHOR INFORMATION

Corresponding Author

*kramm@ese.tu-darmstadt.de

Notes

The authors declare no competing financial interest.

■ ACKNOWLEDGMENTS

Financial support by the DFG funding of the Excellence Initiative, Darmstadt Graduate School of Excellence Energy Science and Engineering (GSC 1070), is gratefully acknowledged by U.I.K. We would like to point out our gratitude for the supply of beamtime at the KMC-2 beamline of BESSY II (HZB) and assistance at the beamline by Alexei Erko. We would like to thank D. Alber and U. Bloeck for NAA and TEM, respectively.

■ REFERENCES

(1) de Frank Bruijn, A.; Janssen, G. J. M. In *Encyclopedia of Sustainable Science and Technology*; Meyers, R. A., Ed.; Springer: New York, 2013; p 7694.

(2) Shui, J.-L.; Chen, C.; Grabstanowicz, L.; Zhao, D.; Liu, D.-J. *Proc. Natl. Acad. Sci. U. S. A.* **2015**, *112*, 10629.

DOI: 10.1021/jacs.5b11015
J. Am. Chem. Soc. 2016, 138, 635−640

(3) Kramm, U. I.; Lefèvre, M.; Larouche, N.; Schmeisser, D.; Dodelet, J.-P. *J. Am. Chem. Soc.* **2014**, *136*, 978.
(4) Wu, G.; More, K. L.; Johnston, C. M.; Zelenay, P. *Science* **2011**, *332*, 443.
(5) Proietti, E.; Jaouen, F.; Lefévre, M.; Larouche, N.; Tian, J.; Herranz, J.; Dodelet, J.-P. *Nat. Commun.* **2011**, *2*, 416.
(6) Serov, A.; Artyushkova, K.; Niangar, E.; Wang, C.; Dale, N.; Jaouen, F.; Sougrati, M. T.; Jia, Q.; Mukerjee, S.; Atanassov, P. *Nano Energy* **2015**, *16*, 293.
(7) Goellner, V.; Baldizzone, C.; Schuppert, A.; Sougrati, M. T.; Mayrhofer, K.; Jaouen, F. *Phys. Chem. Chem. Phys.* **2014**, *16*, 18454.
(8) Jaouen, F.; Herranz, J.; Lefèvre, M.; Dodelet, J.-P.; Kramm, U. I.; Herrmann, I.; Bogdanoff, P.; Maruyama, J.; Nagaoka, T.; Garsuch, A.; Dahn, J. R.; Olson, T. S.; Pylypenko, S.; Atanassov, P.; Ustinov, E. A. *ACS Appl. Mater. Interfaces* **2009**, *1*, 1623.
(9) Zhao, D.; Shui, J.-L.; Grabstanowicz, L. R.; Chen, C.; Commet, S. M.; Xu, T.; Lu, J.; Liu, D.-J. *Adv. Mater.* **2014**, *26*, 1093.
(10) Yuan, S.; Shui, J.-L.; Grabstanowicz, L.; Chen, C.; Commet, S.; Reprogle, B.; Xu, T.; Yu, L.; Liu, D.-J. *Angew. Chem.* **2013**, *125*, 8507.
(11) Sahraie, N. R.; Kramm, U. I.; Steinberg, J.; Zhang, Y.; Thomas, A.; Reier, T.; Paraknowitsch, J. P.; Strasser, P. *Nat. Commun.* **2015**, *6*, 8618.
(12) Liu, S.-H.; Wu, J.-R.; Pan, C.-J.; Hwang, B.-J. *J. Power Sources* **2014**, *250*, 279.
(13) Niwa, H.; Horiba, K.; Harada, Y.; Oshima, M.; Ikeda, T.; Terakura, K.; Ozaki, J.-I.; Miyata, S. *J. Power Sources* **2009**, *187*, 93.
(14) Ferrandon, M.; Wang, X.; Kropf, A. J.; Myers, D. J.; Wu, G.; Johnston, C. M.; Zelenay, P. *Electrochim. Acta* **2013**, *110*, 282.
(15) Yang, J.; Liu, D.-J.; Kariuki, N. N.; Chen, L. X. *Chem. Commun.* **2008**, *3*, 329.
(16) Titov, A.; Zapol, P.; Kral, P.; Liu, D.-J.; Iddir, H.; Baishya, K.; Curtiss, L. A. *J. Phys. Chem. C* **2009**, *113*, 21629.
(17) Ziegelbauer, J. M.; Olson, T. S.; Pylypenko, S.; Alamgir, F.; Jaye, C.; Atanassov, P.; Mukerjee, S. *J. Phys. Chem. C* **2008**, *112*, 8839.
(18) Bron, M.; Radnik, J.; Fieber-Erdmann, M.; Bogdanoff, P.; Fiechter, S. *J. Electroanal. Chem.* **2002**, *535*, 113.
(19) Bouwkamp-Wijnoltz, A. L.; Visscher, W.; van Veen, J. A. R.; Boellaard, E.; van der Kraan, A. M.; Tang, S. C. *J. Phys. Chem. B* **2002**, *106*, 12993.
(20) Müller, K.; Richter, M.; Friedrich, D.; Paloumpa, I.; Kramm, U. I.; Schmeißer, D. *Solid State Ionics* **2012**, *216*, 78.
(21) Herranz, J.; Jaouen, F.; Lefevre, M.; Kramm, U. I.; Proietti, E.; Dodelet, J.-P.; Bogdanoff, P.; Fiechter, S.; Abs-Wurmbach, I.; Bertrand, P.; Arruda, T.; Mukerjee, S. *J. Phys. Chem. C* **2011**, *115*, 16087.
(22) Lefèvre, M.; Dodelet, J.-P.; Bertrand, P. *J. Phys. Chem. B* **2002**, *106*, 8705.
(23) Lefèvre, M.; Dodelet, J.-P.; Bertrand, P. *J. Phys. Chem. B* **2000**, *104*, 11238.
(24) Kramm, U. I.; Lefèvre, M.; Bogdanoff, P.; Schmeißer, D.; Dodelet, J.-P. *J. Phys. Chem. Lett.* **2014**, *5*, 3750.
(25) Matter, P. H.; Wang, E.; Millet, J.-M.; Ozkan, U. S. *J. Phys. Chem. C* **2007**, *111*, 1444.
(26) Schulenburg, H.; Stankov, S.; Schünemann, V.; Radnik, J.; Dorbandt, I.; Fiechter, S.; Bogdanoff, P.; Tributsch, H. *J. Phys. Chem. B* **2003**, *107*, 9034.
(27) Morozan, A.; Sougrati, M. T.; Goellner, V.; Jones, D.; Stievano, L.; Jaouen, F. *Electrochim. Acta* **2014**, *119*, 192.
(28) Zhang, S.; Zhang, H.; Liu, Q.; Chen, S. *J. Mater. Chem. A* **2013**, *1*, 3302.
(29) Kramm, U. I.; Herrmann-Geppert, I.; Fiechter, S.; Zehl, G.; Zizak, I.; Dorbandt, I.; Schmeißer, D.; Bogdanoff, P. *J. Mater. Chem. A* **2014**, *2*, 2663.
(30) Tian, J.; Morozan, A.; Sougrati, M. T.; Lefèvre, M.; Chenitz, R.; Dodelet, J.-P.; Jones, D.; Jaouen, F. *Angew. Chem., Int. Ed.* **2013**, *52*, 6867.
(31) Kramm, U. I.; Herranz, J.; Larouche, N.; Arruda, T. M.; Lefévre, M.; Jaouen, F.; Bogdanoff, P.; Fiechter, S.; Abs-Wurmbach, I.; Mukerjee, S.; Dodelet, J.-P. *Phys. Chem. Chem. Phys.* **2012**, *14*, 11673.
(32) Kramm, U. I.; Herrmann-Geppert, I.; Bogdanoff, P.; Fiechter, S. *J. Phys. Chem. C* **2011**, *115*, 23417.
(33) Kramm, U. I.; Abs-Wurmbach, I.; Herrmann-Geppert, I.; Radnik, J.; Fiechter, S.; Bogdanoff, P. *J. Electrochem. Soc.* **2011**, *158*, B69.
(34) Koslowski, U. I.; Abs-Wurmbach, I.; Fiechter, S.; Bogdanoff, P. *J. Phys. Chem. C* **2008**, *112*, 15356.
(35) Zitolo, A.; Goellner, V.; Armel, V.; Sougrati, M.-T.; Mineva, T.; Stievano, L.; Fonda, E.; Jaouen, F. *Nat. Mater.* **2015**, *14*, 937.
(36) Larouche, N.; Chenitz, R.; Lefèvre, M.; Proietti, E.; Dodelet, J.-P. *Electrochim. Acta* **2014**, *115*, 170.
(37) Maldonado, S.; Stevenson, K. J. *J. Phys. Chem. B* **2005**, *109*, 4707.
(38) Maldonado, S.; Stevenson, K. J. *J. Phys. Chem. B* **2004**, *108*, 11375.
(39) Liu, G.; Li, X.; Ganesan, P.; Popov, B. N. *Electrochim. Acta* **2010**, *55*, 2853.
(40) Liu, G.; Li, X.; Ganesan, P.; Popov, B. N. *Appl. Catal., B* **2009**, *93*, 156.
(41) Nallathambi, V.; Lee, J.-W.; Kumaraguru, S. P.; Wu, G.; Popov, B. N. *J. Power Sources* **2008**, *183*, 34.
(42) Kobayashi, M.; Niwa, H.; Saito, M.; Harada, Y.; Oshima, M.; Ofuchi, H.; Terakura, K.; Ikeda, T.; Koshigoe, Y.; Ozaki, J.-i.; Miyata, S. *Electrochim. Acta* **2012**, *74*, 254−259.
(43) Kobayashi, M.; Niwa, H.; Harada, Y.; Horiba, K.; Oshima, M.; Ofuchi, H.; Terakura, K.; Ikeda, T.; Koshigoe, Y.; Ozaki, J.-i.; Miyata, S.; Ueda, S.; Yamashita, Y.; Yoshikawa, H.; Kobayashi, K. *J. Power Sources* **2011**, *196*, 8346.
(44) Tylus, U.; Jia, Q.; Strickland, K.; Ramaswamy, N.; Serov, A.; Atanassov, P.; Mukerjee, S. *J. Phys. Chem. C* **2014**, *118*, 8999.
(45) Bogdanoff, P.; Herrmann, I.; Hilgendorff, M.; Dorbandt, I.; Fiechter, S.; Tributsch, H. *J. New Mater. Electrochem. Syst.* **2004**, *7*, 85.
(46) Herrmann, I.; Kramm, U. I.; Fiechter, S.; Bogdanoff, P. *Electrochim. Acta* **2009**, *54*, 4275.
(47) Herrmann, I.; Kramm, U. I.; Radnik, J.; Bogdanoff, P.; Fiechter, S. *J. Electrochem. Soc.* **2009**, *156*, B1283.
(48) Ferrandon, M.; Kropf, A. J.; Myers, D. J.; Artyushkova, K.; Kramm, U.; Bogdanoff, P.; Wu, G.; Johnston, C. M.; Zelenay, P. *J. Phys. Chem. C* **2012**, *116*, 16001.
(49) Maruyama, J.; Abe, I. *Chem. Mater.* **2005**, *17*, 4660.
(50) Hu, Y.; Jensen, J. O.; Zhang, W.; Cleemann, L. N.; Xing, W.; Bjerrum, N. J.; Li, Q. *Angew. Chem., Int. Ed.* **2014**, *53*, 3675.
(51) Kuzmann, E.; Nath, A.; Chechersky, V.; Li, S.; Wei, Y.; Chen, X.; Li, J.; Homonnay, Z.; Gál, M.; Garg, V. K.; Klencsár, Z.; Vértes, A. *Hyperfine Interact.* **2002**, *139-140*, 631.
(52) Kramm, U. I. Dr. rer. nat. Thesis, Technische Universität Berlin, 2009.
(53) Hannay, C.; Hubin-Franskin, M.-J.; Grandjean, F.; Briois, V.; Polian, A.; Trofimenko, S.; Long, G. J. *Inorg. Chem.* **1997**, *36*, 5580.
(54) Koslowski, U. I.; Herrmann, I.; Bogdanoff, P.; Barkschat, C.; Fiechter, S.; Iwata, N.; Takahashi, H.; Nishikori, H. *ECS Trans.* **2008**, *13*, 125.

DOI: 10.1021/jacs.5b11015
J. Am. Chem. Soc. 2016, 138, 635−640